

Reactivity of the Uranium(IV) Carbene Complex $[U(BIPM^{TMS})(Cl)(\mu-Cl)_2Li(THF)_2]$ ($BIPM^{TMS} = \{C(PPh_2NSiMe_3)_2\}$) Towards Carbonyl and Heteroallene Substrates: Metallo-Wittig, Adduct Formation, C-F Bond Activation, and [2 + 2]-Cycloaddition Reactions

Oliver J. Cooper,¹ David P. Mills,² William Lewis,¹ Alexander J. Blake,¹ and Stephen T. Liddle*¹

¹ School of Chemistry, University of Nottingham, University Park, Nottingham, NG7 2RD, UK.

² School of Chemistry, University of Manchester, Oxford Road, Manchester, M13 9PL, UK.

*E-mail: stephen.liddle@nottingham.ac.uk

Abstract

*The reactivity of the uranium(IV) carbene complex $[U(BIPM^{TMS})(Cl)(\mu-Cl)_2Li(THF)_2]$ (**1**, $BIPM^{TMS} = \{C(PPh_2NSiMe_3)_2\}$) towards carbonyl and heteroallene substrates is reported. Reaction of **1** with benzophenone proceeds to give the metallo-Wittig terminal alkene product $Ph_2C=C(PPh_2NSiMe_3)_2$ (**2**); the likely “ $UOCl_2$ ” byproduct could not be isolated. Addition of the bulky ketone $PhCOBu^t$ to **1** resulted in loss of $LiCl$, coordination of the ketone, and dimerisation to give $[U(BIPM^{TMS})(Cl)(\mu-Cl)\{OC(Ph)(Bu^t)\}]_2$ (**3**). The reaction of **1** with coumarin resulted in ring opening of the cyclic ester and a metallo-Wittig-type reaction to afford $[U\{BIPM^{TMS}[C(O)(CHCHC_6H_4O-2)]-\kappa^3-N,O,O'\}(Cl)_2(THF)]$ (**4**) where the enolate product remains coordinated to uranium. The reaction of $PhCOF$ with **1** resulted in C-F bond activation and oxidation resulting in isolation of $[U(O)_2(Cl)_2(\mu-Cl)_2\{(\mu-LiDME)OC(Ph)=C(PPh_2NSiMe_3)(PPh_2NHSiMe_3)\}_2]$ (**5**) along with $[U(Cl)_2(F)_2(py)_4]$ (**6**). The reactions of **1** with tert-butylisocyanide or dicyclohexylcarbodiimide resulted in the isolation of the [2 + 2]-cycloaddition products $[U\{BIPM^{TMS}[C(NBu^t)\{OLi(THF)_2(\mu-Cl)Li(THF)_3\}]-\kappa^4-C,N,N',N''\}(Cl)_3]$ (**7**) and $[U\{BIPM^{TMS}[C(NCy)_2]-\kappa^4-C,N,N',N''\}(Cl)(\mu-Cl)_2Li(THF)_2]$ (**8**). Complexes **2-8** have been variously characterised by single crystal X-ray diffraction, multi-nuclear NMR and FTIR spectroscopies, Evans method solution magnetic moments, variable temperature SQUID magnetometry, and elemental analyses.*

Introduction

The first example of a uranium carbene complex, namely $[(\eta^5\text{-C}_5\text{H}_5)_3\text{UC(H)PMe}_2\text{Ph}]$ (**I**), was reported in 1981 by Gilje.¹ A number of reactions of **I**, and the closely related complex $[(\eta^5\text{-C}_5\text{H}_5)_3\text{UC(H)PMe}_3]$ (**II**),² were subsequently reported which included insertion of unsaturated substrates into the U=C bond, but interestingly no reactions with ketones or aldehydes were reported.³ This research area fell into abeyance for nearly thirty years, but was revived within the past five years by a number of research groups including ours.⁴⁻⁷ In recent years the majority of studies have focused on either new methods of preparing U=C double bonds,^{4,5a,7b-d} or expanding the range of U=C double bonds from uranium(IV) to include uranium(V)^{7c,e} and (VI)^{5d,7d} formal oxidation states. Although a small number of metallo-Wittig reactions with simple carbonyl compounds have been reported in recent studies, reactivity data for the U=C double bond linkage remains sparse and the intrinsic reactivity patterns of uranium carbenes has yet to be fully established.^{5a,7c-e} We have made extensive use of the BIPM^{TMS} [BIPM^{TMS} = C(PPh₂NSiMe₃)₂] carbene pincer ligand in f block chemistry,⁸ and in particular have reported a range of reactivity for yttrium analogues.⁹ Of most pertinence to this study, we have found that yttrium BIPM^{TMS} carbene complexes, which are better formulated as methanediides, activate the *ortho*-C-H bonds of aryl ketones to afford C-C and C-O coupled products as opposed to the anticipated metallo-Wittig alkene products.^{9g} To put this into context, the Schrock alkylidene complex $[(\text{Bu}^t\text{CH}_2)_3\text{TaC(H)Bu}^t]$ produces alkenes when reacted with ketones, even with readily enolisable ketones.¹⁰ Preliminary reactivity studies of our uranium BIPM^{TMS} carbenes with a small range of carbonyl compounds, with for example benzaldehyde, afforded the corresponding metallo-Wittig alkene product,^{7c,d} as is the case for closely related SCS-supported [SCS = C(PPh₂S)₂] uranium carbenes,^{5a} which suggests a fundamental difference in the reactivity profiles of uranium and yttrium pincer carbenes/methanediides. We therefore sought to expand the range of carbonyl reactions in a benchmarking study with the uranium(IV) carbene complex $[\text{U}(\text{BIPM}^{\text{TMS}})(\text{Cl})(\mu\text{-Cl})_2\text{Li}(\text{THF})_2]$

(1)^{7c} and report this chemistry herein. In addition, we also report the reactivity of **1** towards isocyanate and carbodiimide heteroallenes.

Results and Discussion

We have previously shown that **1** reacts with 9-anthracene carboxaldehyde to afford the terminal alkene (C₁₄H₁₀)C(H)=C(PPh₂NSiMe₃)₂.^{7c} This is in stark contrast to yttrium analogues which engage in C-H activation of aryl carbonyls to give C-C coupled products.^{9g} Therefore, we investigated the reactivity of **1** towards a range of carbonyl compounds, Scheme 1. The reaction of **1** with benzaldehyde affords the terminal alkene PhC(H)=C(PPh₂NSiMe₃)₂ in 45% isolated yield after recrystallisation and the characterisation data match those previously reported for this olefin.^{7d} Analogously, the reaction of benzophenone with **1** also generates the metallo-Wittig product Ph₂C=C(PPh₂NSiMe₃)₂ (**2**) in 69% crystalline yield, as is the case with SCS-supported uranium carbenes which generate Ph₂C=C(PPh₂S)₂ when treated with benzophenone,^{5a} and the characterisation data support the proposed formulation. In neither case could we isolate the uranium byproduct, but it is most likely an aggregate and/or ligand scrambled moiety of empirical formula UOCl₂. In order to confirm the identity of **2** we determined its structure by X-ray diffraction and the structure is illustrated in Figure 1. The C=C distance of 1.359(4) Å is consistent with the alkene formulation and all other metrical data are unexceptional.¹¹

Benzophenone is relatively bulky compared to 9-anthracene carboxaldehyde and benzaldehyde, reflecting in part their ketone and aldehyde formulations, yet the former still reacts with **1** to give an alkene product so we investigated the potential reaction of the much bulkier *tert*-butyl phenyl ketone with **1**, Scheme 1. Accordingly, **1** was treated with one equivalent of *tert*-butyl phenyl ketone, but rather than a metallo-Wittig reaction occurring we find that instead only the adduct formulated as [U(BIPM^{TMS})(Cl)(μ-Cl){OC(Ph)(Bu^t)}₂ (**3**) could be isolated in 37% crystalline yield. Heating reaction mixtures did not promote alkene formation with only decomposition being

observed after prolonged heating. Inspection of the NMR spectra of the crystals did not suggest the isolation of an alkene product, and the ^1H NMR spectrum suggested the loss of THF and incorporation of PhCOBu^\dagger . To confirm the nature of **3** an X-ray diffraction study was undertaken and the structure is illustrated in Figure 2.

Complex **3** is dimeric in the solid state with a PhCOBu^\dagger molecule coordinating to each uranium centre instead of reacting across the $\text{U}=\text{C}$ bond in a metallo-Wittig manner, whilst the occluded LiCl of **1** has been lost. The U1-C1 bond distance in **3** [2.346(4) Å] is 0.03 Å longer than the equivalent bond length in **1** [2.310(4) Å].^{7c} The terminal U1-Cl2 bond distance in **3** [2.6223(10) Å] is comparable to that in **1** [2.6249(13) Å], however the bridging U1-Cl1 bond distance in **3** [2.8471(9) Å] is ~ 0.1 Å longer than both those reported in **1**. Complex **3** exhibits lengthening of the U-N bond distances by ~ 0.06 Å compared to those seen in **1**, whilst the P-N bond distances are statistically equivalent. The P1-C1-P2 bond angle in **3** [144.6(3)°] is smaller than the corresponding angle in **1** [164.8(3)°]. This may be due to either the removal of a halide and the coordination of a ketone or due to **3** being dimeric affecting the planarity of the carbene ligand by forcing the ligand towards an ‘open-book’ conformation.^{7e}

The coordination of a ketone to uranium raises the possibility that **3** could be formulated as a pentavalent uranium complex with a PhCOBu^\dagger ketyl radical anion.¹² However, the metric data of the crystal structure are consistent with a tetravalent assignment,¹¹ since the O1-C32 bond length [1.239(6) Å] is typical for a $\text{C}=\text{O}$ double bond and lies within the sum of the covalent radii of doubly bonded carbon and oxygen (1.24 Å).¹³ Furthermore, the yellow colour of **3** is not consistent with a ketyl radical which would be expected to be dark blue or purple in colour. The magnetism of **3** is indicative of uranium(IV) with a solution magnetic moment of $3.93 \mu_{\text{B}}$, whilst in the solid state the magnetic moment is $4.28 \mu_{\text{B}}$ at 300 K, which decreases to $0.47 \mu_{\text{B}}$ at 1.8 K and clearly tends towards zero, Figure 3a. We find no evidence of magnetic communication between the two uranium

centres in **3**, which is not unexpected since magnetic communication between uranium(IV) centres is very rare.¹⁴ The room temperature solid state magnetic moment in **3** is significantly higher than that observed in **1** (2.62 μ_B), due to the former being dimeric.

Since the sterically demanding ketone PhCOBu^t does not undergo Wittig-type reactivity towards **1**, and only coordinates to the uranium centre, we conclude that the steric bulk of the ketone plays a significant role in determining whether Wittig-type reactions are kinetically viable or not. It should be noted, however, that **3** represents the initial stages of a reaction between **1** and a ketone since coordination of carbonyl compounds to the metal centre has been observed by us before,^{7e} and had been postulated previously as the first step in metallo-Wittig reactions.¹⁰

Having established a kinetic boundary on the reactivity of **1** towards carbonyl compounds, we investigated the reactivity of the cyclic ester coumarin towards **1**. The reaction between **1** and coumarin afforded the enolate-aryloxide complex [U{BIPM^{TMS}[C(O)(CHCHC₆H₄O-2)]- κ^3 -*N,O,O'*}_2(Cl)₂(THF)] (**4**) as yellow crystals in 25% yield, Scheme 1. The ¹H NMR spectrum of **4** reveals a sixteen line spectrum spanning the range from -10.64 to 13.62 ppm, suggesting the incorporation of coumarin into the structure. To confirm the identity of **4** an X-ray diffraction study was undertaken.

Complex **4** is monomeric in the solid-state and the uranium centre adopts a distorted octahedral geometry (Figure 4). The carbene has nucleophilically attacked the ester carbon resulting in ring-opening and ultimately the formation of an enolate and aryloxide; there is no uranium carbon bond in **4** and only one of the nitrogen atoms on the BIPM^{TMS} scaffold is coordinated to uranium. The two oxygen atoms in the coumarin molecule are now bonded to uranium, which is reflected by the U1-O1 and U1-O2 bond distances in **4** [2.089(3) and 2.213(3) Å respectively], which are shorter than the U1-O3 bond distance in **4** [2.416(4) Å] of the coordinated THF molecule, and at the lower

end of reported U-O bond distances (1.757–2.90 Å).¹¹ The O1 centre can formally be attributed as anionic while there is delocalisation across the C1-C32-O2 bonds. The C1–C32 bond distance in **4** [1.361(7) Å] is consistent with a C=C double bond and is comparable to the C=C bond length in **2**. The O2-C32 bond distance in **4** [1.335(6) Å] is also consistent with partial carbonyl C=O character. The U1-N2 bond distance in **4** [2.394(4) Å] is statistically indistinguishable to the mean U-N bond lengths in **1** [2.3725(4) Å], whilst the mean C-P bond distances in **4** are ~0.15 Å longer than the equivalent bond lengths in **1** [2.3725(4) Å]. The P1-N1 bond distance in **4** [1.541(4) Å] is 0.07 Å shorter than the P2-N2 bond distance in **4** [1.616(4) Å] which is a reflection of N1 not coordinating to uranium and being pendant.

The infrared spectrum exhibits C-O stretches at 1052 and 1026 cm⁻¹, and a C=C stretch at 1619 cm⁻¹ supporting the proposed formulation. The solution magnetic moment of **4** is 2.51 μ_B; in the solid state the magnetic moment in **4** is 2.17 μ_B at 300 K, and this decreases to 0.41 μ_B at 1.8 K and clearly tends towards zero, Figure 3b. This is consistent with the presence of a uranium(IV) centre.

We next investigated the reactivity of **1** towards PhCOF since we previously demonstrated that the yttrium analogue of **1**, [Y(BIPM^{TMS})(I)(THF)₂] activated the C-F bond to afford half a molar equivalent of the enolate complex [Y{C(PPh₂NSiMe₃)₂[C(O)(Ph)]-κ²-N,O}₂(I)] with concomitant formal elimination of half a molar equivalent of “YF₂I(THF)_n”.^{9h} Treatment of **1** with PhCOF resulted in the formation of two complexes which could be separated by fractional crystallisation, albeit in low yields, Scheme 1. Recrystallisation of the DME extract of the reaction afforded crystals of [U(O)₂(Cl)₂(μ-Cl)₂{(μ-LiDME)OC(Ph)=C(PPh₂NSiMe₃)(PPh₂NHSiMe₃)₂}₂] (**5**) in 24% yield. Extracting the remaining solid obtained from initial work up with THF and recrystallisation from pyridine gave crystals of [U(Cl)₂(F)₂(py)₄] (**6**) in 36% yield. Although the yields of **5** and **6** are low their isolation permits us to understand the reactivity that is occurring. The reaction of **1** with benzoyl fluoride is only the second example of a report of the reactivity of this acyl halide with an

early metal carbene.^{9h} Previously, it has been postulated that the carbonyl group pre-coordinates to the metal, which is supported by the isolation of **3**, then the carbene nucleophilically attacks the electrophilic ketyl carbon and via a [2 + 2]-cycloaddition and bond metathesis cleaves the C-F bond to generate a M-F bond and an enolate; we suggest a similar mechanism operates here. Additionally, during the formation of **5** comproportionation must occur. The isolation of **6** is notable because the uranium byproducts from Wittig reactions are not normally isolable. The characterisation data for **5** support the proposed formulation. In particular, the presence of an N-H group is suggested by a broad band in the FTIR spectrum at 3386 cm⁻¹, and a stretch at 930 cm⁻¹ is consistent with the presence of a uranyl group. It should be noted that from a stoichiometric perspective, the formation of **5** and **6** accounts for all the mass balance except for the two uranyl oxos and the two protons; we surmise that oxidation of uranium(IV) to (VI) occurs during the reaction, but we could not ascertain the oxo or proton sources. Since the yields are low, these atoms could originate from PhCOF as well as adventitious oxygen or moisture. However, we note that since one imino arm of each BIPM^{TMS} fragment is protonated this suggests that trace water may be the source of oxo and protons, but attempts to spike reaction mixtures with water resulted in intractable mixtures.

The molecular structures of **5** and **6** were determined by X-ray crystallography and are illustrated in Figures 5 and 6. The structure of **5** is composed of a uranyl(VI) centre which is coordinated by four chloride ligands in a square-based bipyramid geometry. Two of the chlorides in this formally dianionic UO₂Cl₄ unit bridge to lithium cations which are in turn each coordinated to a molecule of DME solvent and the oxygen centre of the enolate derivative of BIPM^{TMS} from the [2 + 2] cycloaddition reaction. The O1–C32 and C1–C32 bond lengths [1.269(8) and 1.416(9) Å, respectively] are shorter and longer than the analogous bond lengths in **4** but are not fully consistent with localised double and single bonds so it is concluded that there is some delocalisation within the OCC unit of **5**. Notably, the N1–P1 and N2–P2 bond lengths [1.562(5) and 1.641(6) Å, respectively]

are significantly different; the longer N2–P2 distance suggests protonation which is confirmed by inspection of the difference electron density map which reveals that the N2 atom is protonated which provides charge balance for this aggregate. All other bond lengths and angles are unremarkable. The structure of **6** confirms the fate of the eliminated uranium fragment from **5** and is notable for being fully ordered, which might not be expected given the polar nature of these uranium-halide bonds.

We next turned our attention to the reactivity of the isocyanate functional group. The reaction between **1** and Bu^tNCO afforded [U{BIPM^{TMS}[C(NBu^t){OLi(THF)₂(μ-Cl)Li(THF)₃}]-κ⁴-C,N,N',N''(Cl)₃] (**7**) as green crystals in 25% yield, Scheme 1. Although a [2 + 2]-cycloaddition reaction has occurred, it is notable that both imino arms and the central carbon atom of the BIPM^{TMS} ligand remain coordinated; this contrasts to the reactions of **I** and **II** with PhNCO where the U=C bond was completely ruptured which reflects that in the former the carbene is constrained in a pincer chelate arrangement whereas for **I** and **II** the U=C linkage is unsupported.^{2,3} The ¹H NMR spectrum and elemental analysis of **7** indicate that the bulk of the sample does not possess the second {LiCl(THF)₃} fragment, which is observed in the solid state structure of **7** shown in Figure 7, and the bulk is formulated as [U{BIPM^{TMS}[C(NBu^t){OLi(THF)₂}] -κ⁴-C,N,N',N''(Cl)₃] according to CHN analysis.

The seven coordinate uranium centre in **7** adopts a distorted pentagonal bipyramidal conformation, with the isocyanate having undergone [2 + 2] cycloaddition across the U=C bond, with the nitrogen bonding to uranium to form a U-N bond. This is comparable to [Zr{BIPM^{TMS}[C(O)(NAd)]-κ⁴-C,N,N',N''(Cl)₂}]¹⁵ but contrasts to [Y{BIPM^{TMS}[C(O)(NBu^t)]-κ⁴-C,N,N',O}{C(O)(NBu^t)(CH₂Ph)-κ²-N,O}], which forms an Y-O bond.⁹ⁱ This variation can be attributed to the HSAB principle, with the hard yttrium having a greater affinity towards the hard oxygen,¹⁶ and although uranium has a high oxophilicity, meaning a U-O bond would be expected

over a U-N bond, the coordination of the oxygen by lithium may remove electron density away from the oxygen atom decreasing its hardness. Alternatively, the coordination of lithium to oxygen may sterically block the oxygen bonding to uranium.

The BIPM^{TMS} ligand in **7** adopts an ‘open-book’ conformation which is evidenced by the P1-C1-P2 angle of 126.83(17)°, and is larger than the corresponding angle in **8** [121.2(3)°, see below]. The U1-C1 bond length in **7** [2.634(3) Å] is shorter than the U-C bond in **8** [2.712(5) Å, see below]. The C1-C32 bond distance in **7** [1.512(4) Å] is consistent with a C-C single bond and is statistically indistinguishable to the equivalent bond length in **8** [1.525(7) Å, see below]. The O1-C32 bond distance in **7** [1.242(4) Å] is about the sum of the covalent radii for a C=O double bond (1.24 Å) whilst the N3-C32 bond length in **7** [1.334(4) Å] lies in between the covalent radii of a C-N single (1.46 Å) and C=N double bond (1.27 Å),¹³ suggesting a degree of delocalisation across the O1-C32-N3 linkage. The U1-N3 bond distance in **7** [2.451(3) Å] is long suggesting a more dative interaction, which would require the uranium centre in **7** to be in the +4 oxidation state. The tetravalent nature of **7** is confirmed by inspection of the magnetic moment of **7**, which in solution is 2.59 μ_B; in the solid state the magnetic moment in **7** is 3.27 μ_B at 300 K, and this decreases to 0.31 μ_B at 1.8 K and clearly tends towards zero, Figure 3c.

The reactions reported thus far have involved unsaturated compounds with carbonyl functionalities, to deviate from this our attention turned towards carbodiimides. The reaction between **1** and C(NCy)₂ yielded [U{BIPM^{TMS}[C(NCy)₂]-κ⁴-C,N,N',N''}(Cl)(μ-Cl)₂Li(THF)₂] (**8**) as green crystals in 42% yield, Scheme 1. Again, like **7**, the uranium-imino and -central carbon bonds remain intact perhaps reflecting the constraints of the pincer chelate. The characterisation data is consistent with the formulation of **8**, with the solid state structure of **8** shown in Figure 8.

Complex **8** is monomeric in the solid state, with the uranium centre adopting a distorted pentagonal bipyramidal conformation, and is coordinated by an occluded lithium chloride fragment. The carbodiimide has undergone [2 + 2] cycloaddition across the U=C bond, akin to the reactions reported by Cavell between “[U(BIPM^{TMS})(Cl)₂]” and acetonitrile or benzonitrile, which gave the [2 + 2] cycloaddition products [(BIPM^{TMS})ClU(μ-Cl)₂UCl{NC(R)C(PPh₂NSiMe₃)-κ⁴-C,N,N',N''}] (R = Me or Ph).⁶ The [2 + 2] cycloaddition of the carbodiimide closely resembles that of transition metal and lanthanide BIPM carbene complexes, with [Zr{BIPM^{TMS}(C[NCy]₂)-κ⁴-C,N,N',N''}(Cl)₂] and [Y{BIPM^{TMS}(C[NCy]₂)-κ⁴-C,N,N',N''}{C-(NCy)₂(CH₂Ph)-κ²-N,N'}],¹⁵ respectively, being reported. The BIPM^{TMS} ligand in **8** adopts an ‘open-book’ conformation which is evidenced by the P1-C1-P2 angle of 121.2(3)°, which is smaller than the corresponding angle in **3**. The U1-C1 bond length in **8** [2.712(5) Å] is similar to other uranium methanide bond lengths.¹¹

The C1-C32 bond distance in **8** [1.525(7) Å] is typical for a C-C single bond, and lies just outside the covalent radii of a C-C bond (1.50 Å).¹³ The N3-C32 bond distance in **8** [1.273(6) Å] is relatively short, whilst the N4-C32 bond distance [1.388(6) Å] is longer and suggests localised double and single bonds respectively. The U1-N4 bond length [2.296(4) Å] and the U1-N1 and U1-N2 bond distances in **8** [2.456(4) and 2.376(4) Å, respectively] are consistent with previously reported U(IV)-N bond distances,¹⁷ whilst these bond lengths suggest the U1-N4 is a single covalent bond compared to the U1-N1 and U1-N2 bonds which are more dative in nature. The tetravalent nature of **8** is confirmed upon inspection of the magnetic moment of **8** in solution which is 2.57 μ_B; in the solid state the magnetic moment in **8** is 2.64 μ_B at 300 K, and this decreases to 0.22 μ_B at 1.8 K and clearly tends towards zero, Figure 3d.

Conclusions

We have examined the reactivity of the uranium(IV) carbene complex **1** towards a range of unsaturated substrates. What emerges from these studies is that metallo-Wittig reactivity to generate

alkenes, be they free terminal alkenes or enolate-type derivatives which remain coordinated to uranium or occluded lithium chloride, dominates and there is no evidence for more aggressive C-H activation reactions that occurs readily for yttrium analogues that are more appropriately formally described as methanediides. Where the ketone is too sterically demanding only an adduct forms presumably due to kinetic factors, but this can be viewed as the first step in a metallo-Wittig reaction. However, facile C-F bond activation is observed in one case which together with the enolate reactions underscores the oxo- and halophilic nature of uranium(IV). Heteroallenes undergo [2 + 2]-cycloaddition reactions but these reactions do not proceed to the hypothetical next step of σ -bond metathesis to liberate ketenimine derivatives; this presumably is due to the chelate pincer nature of the BIPM^{TMS} carbene where too many uranium-element bonds would have to be cleaved to effect metallo-Wittig reactivity. We are continuing to investigate the reactivity of uranium BIPM^{TMS} carbenes with oxidation states of IV-VI for uranium and will report on this in due course.

Experimental

General

All manipulations were carried out using standard Schlenk techniques, or an MBraun UniLab glovebox, under an atmosphere of dry nitrogen. Solvents were dried by passage through activated alumina towers and degassed before use. All solvents were stored over potassium mirrors (with the exception of THF which was stored over activated 4 Å molecular sieves). Deuterated solvents were distilled from potassium, degassed by three freeze-pump-thaw cycles and stored under nitrogen. All other chemicals were purchased and all solid reagents were dried under vacuum for four hours and all liquid reagents were dried over 4 Å molecular sieves and distilled before use. ¹H, ⁷Li, ¹³C, ²⁹Si, and ³¹P NMR spectra were recorded on a Bruker 400 spectrometer operating at 400.2, 128.4, 100.6, 79.5, and 162.0 MHz, respectively; chemical shifts are quoted in ppm and are relative to TMS (¹H, ¹³C and ²⁹Si) and external 1M LiCl (⁷Li) or 85% H₃PO₄ (³¹P). FTIR spectra were recorded on a Bruker Tensor 27 spectrometer. Variable-temperature magnetic moment data for **3**, **4**, and **7-8** were

recorded in an applied dc field of 0.1 T on a Quantum Design MPMS XL5 SQUID magnetometer using doubly recrystallised powdered samples suspended in eicosane. Care was taken to ensure complete thermalisation of the sample before each data point was measured. Diamagnetic corrections were applied for **3**, **4**, and **7-8** using tabulated Pascal constants and measurements were corrected for the effect of the blank sample holders (flame sealed Wilmad NMR tube and straw). Elemental microanalyses were carried out by Dr Tong Liu at the University of Nottingham. Complex **1** was prepared as described previously.^{7c}

Preparation of PhC(H)=C(PPh₂NSiMe₃)₂

PhCHO (0.11 g, 1.00 mmol) in toluene (10 ml) was added to a solution of **1** (1.09 g, 1.00 mmol) in toluene (10 ml). The solution was stirred for 66 hours to give a grey reaction mixture. The mixture was filtered and volatiles removed *in vacuo* to afford a pale grey solid. Recrystallisation from acetonitrile afforded colourless crystals of PhC(H)=C(PPh₂NSiMe₃)₂. Yield: 0.29 g, 45%. Characterisation data matched those previously reported.

Preparation of Ph₂C=C(PPh₂NSiMe₃)₂ (2)

Ph₂CO (0.18 g, 1.00 mmol) in toluene (10 ml) was added to a solution of **1** (1.09 g, 1.00 mmol) in toluene (10 ml). The solution was stirred for 66 hours to give a grey reaction mixture. The mixture was filtered and volatiles removed *in vacuo* to afford a pale grey solid. Recrystallisation from acetonitrile afforded colourless crystals of **2**. Yield: 0.50 g, 69%. Anal Calcd for C₄₄H₄₈N₂P₂Si₂: C, 73.10; H, 6.70; N, 3.88%. Found: C, 73.12; H, 6.74; N, 3.76%. ¹H NMR (C₆D₆, 298 K): δ 0.79 (s, 18H, SiCH₃), 6.92-7.00 (m, br, 16H, Ar-H), 7.28 (m, br, 2H, Ar-H), 7.41 (m, br, 4H, Ar-H), 7.95 (m, br, 8H, Ar-H). ¹³C {¹H} NMR (C₆D₆, 298 K): δ 4.80 (SiCH₃), 126.79, 127.28, 128.30, 129.51, 131.73, 136.26 (t, *J*_{PC} = 145.87 Hz), 137.39, 138.58 (dd, *J*_{PC} = 119.76 Hz, ³*J*_{PC} = 14.09 Hz, *C*_{ipso}), 143.76 (t, ³*J*_{PC} = 12.08 Hz, *C*_{ipso}), 176.31 (CPh₂). ³¹P NMR (C₆D₆, 298 K): δ 8.18. ²⁹Si NMR (C₆D₆, 298 K): δ -17.22 (vt, ²*J*_{psi} = 15.07 Hz). FTIR ν/cm⁻¹ (Nujol): 1666 (w), 1614 (w), 1316 (m), 1261

(m), 1238 (m), 1155 (w), 1097 (m), 1027 (m), 985 (m), 916 (m), 862 (m), 824 (m), 802 (m), 766 (m), 748 (m), 721 (m), 637 (w), 584 (w), 546 (w), 517 (m), 496 (m), 455 (m), 422 (m).

Preparation of $[U(BIPM^{TMS})(Cl)(\mu-Cl)\{OC(Ph)(Bu^t)\}]_2$ (3)

PhCO^tBu (0.16 g, 1.00 mmol) in toluene (10ml) was added to pre-cooled (−78 °C) **1** (1.09 g, 1.00 mmol) in toluene (10ml), which upon returning to room temperature was stirred for a further 18 hours to afford a dark brown solution. Volatiles were removed *in vacuo* and the resulting brown solid was recrystallised from toluene (10 ml) to afford **3** as yellow crystals. Yield: 0.38 g, 37%. Anal Calcd for C₄₂H₅₂Cl₂N₂OP₂Si₂U·0.5C₇H₈: C, 50.87; H, 5.26; N, 2.61%. Found: C, 50.84; H, 5.24; N, 2.59%. ¹H NMR (C₆D₆, 298 K): δ 0.42 (s, 2H, Ar-*H*), 1.08 (s, 9H, C(CH₃)₃), 1.76 (s, 4H, Ar-*H*), 2.236 (s, 2H, Ar-*H*), 3.74 (s, 2H, Ar-*H*), 5.56 (s, 1H, *p*-Ar-*H*), 7.15 (s, 4H, Ar-*H*), 7.67 (s, 4H, Ar-*H*), 11.72 (v br, 18H, Si(CH₃)₃), 18.26 (s, 4H, Ar-*H*). FTIR ν/cm^{-1} (Nujol): 1614 (s), 1589 (m), 1571 (m), 1245 (s), 1182 (m), 1107 (s), 1049 (s). (Evans method, C₆D₆, 298 K): 3.93 μ_B .

Preparation of $[U\{BIPM^{TMS}[C(O)(CHCHC_6H_4O-2)]-\kappa^3-N,O,O'\}(Cl)_2(THF)]$ (4)

THF (20 ml) was added to a pre-cooled (−78 °C) mixture of **1** (1.09 g, 1.00 mmol) and coumarin (0.15 g, 1.00 mmol). The reaction mixture was slowly allowed to warm to room temperature with stirring over 24 h. The mixture was filtered, reduced in volume to *ca.* 4 ml and stored at 4 °C overnight to afford **4** as yellow crystals. Two further crops were obtained. Yield: 0.31 g, 25 %. Anal Calcd for C₄₄H₅₂Cl₂N₂O₅P₂Si₂U: C, 47.34; H, 4.70; N, 2.51%. Found: C, 44.62; H, 4.59; N, 2.32%. Low carbon is ascribed to carbide formation.^x ¹H NMR (C₆D₆, 298 K): δ −10.64 (s, br, 4H, OCH₂CH₂), −8.30 (s, br, 4H, OCH₂CH₂), −4.76 (s, 1H, Ph-*CH*), −3.70 (s, 1H, Ph-*CH*), −3.16 (s, 1H, Ph-*CH*), −2.68 (br, 4H, Ph-*CH*), −2.40 (s, 1H, Ph-*CH*), −2.09 (s, 1H, CH=CH), −1.96 (s, 1H, CH=CH), 0.42 (s, br, 4H, Ph-*CH*), 1.12 (s, br, 9H, Si(CH₃)₃), 2.82 (s, br, 4H, Ph-*CH*), 3.02 (s, br, 9H, Si(CH₃)₃), 5.91 (s, br, 4H, Ph-*CH*), 12.24 (s, 2H, *p*-Ph-*CH*), 13.62 (s, 2H, *p*-Ph-*CH*). FTIR

ν/cm^{-1} (Nujol): 3055 (m, =C-H), 1619 (w, C=C), 1260 (s), 1052 (s, C-O), 1026 (s, C-O). μ_{eff} (Evans method, C_6D_6 , 298 K): 2.51 μ_{B} .

Preparation of $[\text{U}(\text{O})_2(\text{Cl})_2(\mu\text{-Cl})_2\{(\mu\text{-LiDME})\text{OC}(\text{Ph})=\text{C}(\text{PPh}_2\text{NSiMe}_3)(\text{PPh}_2\text{NHSiMe}_3)\}_2]$ (5) and $[\text{U}(\text{Cl})_2(\text{F})_2(\text{py})_4]$ (6)

PhCOF (0.12 g, 1.00 mmol) in toluene (10 ml) was added dropwise to a pre-cooled ($-78\text{ }^\circ\text{C}$) suspension of **1** (1.09 g, 1.00 mmol) in toluene (10 ml). The reaction mixture was slowly allowed to warm to room temperature with stirring over 24 h. Volatiles were removed in vacuo and the product was extracted into DME (2 ml) and stored at ambient temperature overnight to afford **5** as colourless crystals. Yield: 0.24 g, 24 %. Anal Calcd for $\text{C}_{84}\text{H}_{108}\text{Cl}_4\text{Li}_2\text{N}_4\text{O}_8\text{P}_4\text{Si}_4\text{U}$: C, 52.23; H, 5.64; N, 2.90%. Found: C, 52.56; H, 5.83; N, 2.62%. ^1H NMR (d_6 -benzene, 298 K): δ -0.06 (s, 16H, Ph-CH), 1.70 (s, 2H, *p*-Ph-CH), 3.23 (s, 4H, Ph-CH), 3.43 (s, 8H, Ph-CH), 3.65 (s, br, 36H, $\text{Si}(\text{CH}_3)_3$), 3.84 (s, 4H, Ph-CH), 6.72 (s, 8H, OCH_2), 7.30 (s, 16H, Ph-CH), 8.13 (s, 12H, OCH_3). $^{31}\text{P}\{^1\text{H}\}$ NMR (d_6 -benzene, 298 K): δ 27.67 (s, br). $^7\text{Li}\{^1\text{H}\}$ NMR (d_6 -benzene, 298 K): δ 2.00 (s, br). FTIR ν/cm^{-1} (Nujol): 3386 (br), 1589 (w), 1576 (w), 1521 (m), 1304 (m), 1233 (m), 1156 (m), 1106 (s), 1087 (s), 1020 (s), 979 (m), 930 (m), 869 (m), 842 (s), 822 (m), 778 (m), 748 (m), 734 (m), 693 (m), 600 (w), 574 (w), 556 (w), 536 (w), 505 (w). The remainder was treated with THF (5 ml), volatiles were removed and the residue extracted with pyridine (1 ml) and stored at $5\text{ }^\circ\text{C}$ overnight to afford **6** as green crystals. Yield 0.24 g, 36 %. This sample was impure, precluding further analysis.

Preparation of $[\text{U}\{\text{BIPM}^{\text{TMS}}[\text{C}(\text{NBu}^t)\{\text{OLi}(\text{THF})_2(\mu\text{-Cl})\text{Li}(\text{THF})_3\}]\text{-}\kappa^4\text{-C,N,N',N''}\text{-}(\text{Cl})_3]$ (7)

Toluene (10 ml) was added to a pre-cooled ($-78\text{ }^\circ\text{C}$) mixture of **1** (1.09 g, 1.00 mmol) and $^t\text{BuNCO}$ (0.099 g, 1.00 mmol). The mixture was then allowed to slowly warm to room temperature with stirring over 18 hours to afford a dark green solution. The solution was filtered and volatiles were then removed *in vacuo*. The resulting green solid was recrystallised from a mixture of THF and

^tBuOMe to afford **7** as green crystals. Yield: 0.38g, 25%. Anal Calcd for C₃₉H₅₅Cl₃LiN₃O₃P₂Si₂U: C, 43.89; H, 5.19; N, 3.94%. Found: C, 43.53; H, 5.34; N, 3.81%. ¹H NMR (*d*₈-THF, 298 K): δ - 1.17 (s, 18H, Si(CH₃)₃), 0.14 (s, 9H, C(CH₃)₃), 1.82 (m, 8H, THF), 3.66 (m, 8H, THF), 5.78 (s, 4H, *p*-Ar-CH), 7.32-7.97 (m, 16H, Ar-CH). FTIR ν/cm⁻¹ (Nujol): 1552 (m), 1315 (w), 1255 (w), 1108 (m), 1038 (m), 845 (m), 774 (w). (Evans method, C₆D₆, 298 K): 2.59 μ_B.

Preparation of [U{BIPM^{TMS}[C(NCy)₂]-κ⁴-C,N,N',N'}(Cl)(μ-Cl)₂Li(THF)₂] (8**)**

Toluene (10 ml) was added to a pre-cooled (-78 °C) mixture of **1** (1.09 g, 1.00 mmol) and C(NCy)₂ (0.128g, 1.00 mmol). The mixture was then allowed to slowly warm to room temperature with stirring over 18 hours to afford a dark green solution. The solution was filtered and volatiles were then removed *in vacuo*. The resulting green solid was recrystallised from a mixture of THF and ^tBuOMe to afford **8** as green crystals. Yield: 0.53g, 42%. Anal Calcd for C₅₂H₇₆Cl₃LiO₂N₄P₂Si₂U·2THF: C, 51.34; H, 6.48; N, 4.00%. Found: C, 50.99; H, 6.89; N, 4.35%. ¹H NMR (*d*₈-THF, 298 K): δ -6.33 (s, 18H, Si(CH₃)₃), -1.89 (br, 8H), -1.70, (s, 8H), -0.58 (s, 8H), 2.21 (br, 4H), 3.81 (s, 2H, CH₂-Cy), 4.67 (s, 2H, CH₂-Cy), 5.27 (s, 4H, CH₂-Cy), 5.47 (s, 2H, CH₂-Cy), 5.62 (s, 4H, CH₂-Cy), 6.30 (s, 1H, NCH-Cy), 6.64 (s, 1H, NCH-Cy), 7.00 (br, 8H), 8.03 (s, 2H, CH₂-Cy), 8.92 (s, 2H, CH₂-Cy), 10.35 (s, 2H, CH₂-Cy). FTIR ν/cm⁻¹ (Nujol): 3055 (w), 1580 (m), 1439 (s), 1247 (m), 1212 (w), 1108 (m), 1055 (s), 1003 (m), 842 (m). μ_{eff} (Evans method, C₆D₆, 298 K): 2.57 μ_B.

Acknowledgement

We gratefully acknowledge generous support of this work by the Royal Society, EPSRC, ERC, the University of Nottingham, and the UK National Nuclear Laboratory.

Electronic Supplementary Information

X-ray crystallographic data for **2-8**. CCDC 993178-993184.

References

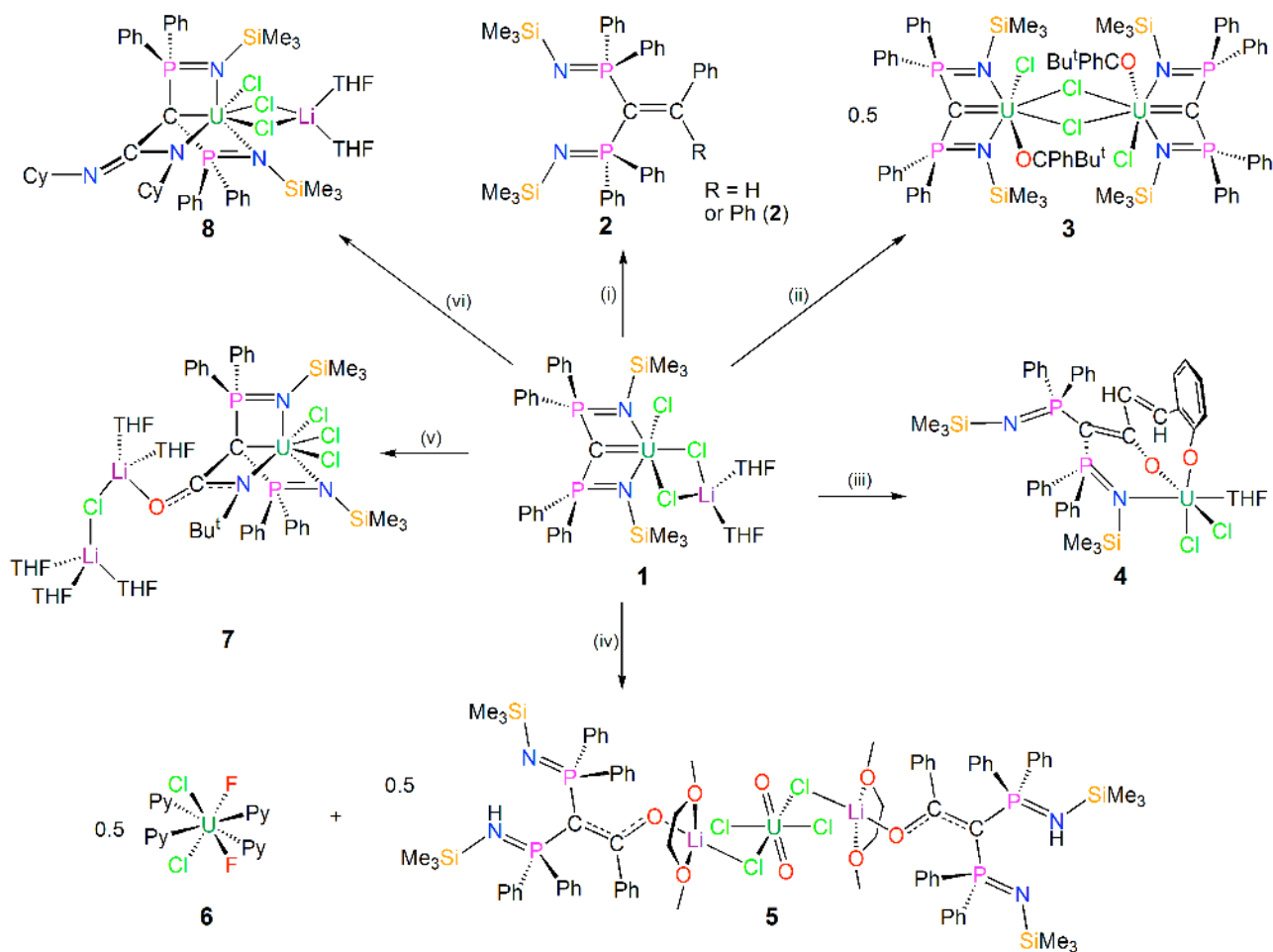
1. R. E. Cramer, R. B. Maynard, J. C. Paw, J. W. Gilje, *J. Am. Chem. Soc.*, 1981, **103**, 3598.
2. a) R. E. Cramer, R. B. Maynard, J. W. Gilje, *Inorg. Chem.*, 1981, **20**, 2466; b) J. W. Gilje, R. E. Cramer, *Inorg. Chim. Acta*, 1987, **139**, 177.
3. a) R. E. Cramer, R. B. Maynard, J. C. Paw, J. W. Gilje, *Organometallics*, 1982, **1**, 869; b) R. E. Cramer, K. T. Higa, S. L. Pruskin, J. W. Gilje, *J. Am. Chem. Soc.*, 1983, **105**, 6749; c) R. E. Cramer, K. Panchanatheswaran, J. W. Gilje, *Angew. Chem. Int. Ed.*, 1984, **23**, 912; d) R. E. Cramer, K. Panchanatheswaran, J. W. Gilje, *J. Am. Chem. Soc.*, 1984, **106**, 1853; e) R. E. Cramer, K. T. Higa, J. W. Gilje, *J. Am. Chem. Soc.*, 1984, **106**, 7245; f) R. E. Cramer, J. H. Jeong, J. W. Gilje, *Organometallics*, 1986, **5**, 2555; g) R. E. Cramer, J. H. Jeong, J. W. Gilje, *Organometallics*, 1987, **6**, 2010; h) R. E. Cramer, J. H. Jeong, P. N. Richmann, J. W. Gilje, *Organometallics*, 1990, **9**, 1141.
4. S. Fortier, J. R. Walensky, G. Wu, T. W. Hayton, *J. Am. Chem. Soc.*, 2011, **133**, 6894.
5. a) T. Cantat, T. Arliguie, A. Noël, P. Thuéry, M. Ephritikhine, P. Le Floch, N. Mézailles, *J. Am. Chem. Soc.*, 2009, **131**, 963; b) J. C. Tourneux, J. -C. Berthet, P. Thuéry, N. Mézailles, P. Le Floch, M. Ephritikhine, *Dalton Trans.*, 2010, **39**, 2494; c) J. -C. Tourneux, J. -C. Berthet, T. Cantat, P. Thuéry, N. Mézailles, P. Le Floch, M. Ephritikhine, *Organometallics*, 2011, **30**, 2957; d) J. C. Tourneux, J. -C. Berthet, T. Cantat, P. Thuéry, N. Mézailles, M. Ephritikhine, *J. Am. Chem. Soc.*, 2011, **133**, 6162; e) M. Ephritikhine, *Comptes Rendu. Chimie*, 2013, **16**, 391.
6. G. Ma, M. J. Ferguson, R. McDonald, R. G. Cavell, *Inorg. Chem.*, 2011, **50**, 6500.
7. a) O. J. Cooper, J. McMaster, W. Lewis, A. J. Blake, S. T. Liddle, *Dalton Trans.*, 2010, **39**, 5074; b) D. P. Mills, F. Moro, J. McMaster, J. Van Slageren, W. Lewis, A. J. Blake, S. T. Liddle, *Nat. Chem.*, 2011, **3**, 454; c) O. J. Cooper, D. P. Mills, J. McMaster, F. Moro, E. S. Davies, W. Lewis, A. J. Blake, S. T. Liddle, *Angew. Chem. Int. Ed.*, 2011, **50**, 2383; d) D. P. Mills, O. J. Cooper, F. Tuna, E. J. L. McInnes, E. S. Davies, J. McMaster, F. Moro, W.

- Lewis, A. J. Blake, S. T. Liddle, *J. Am. Chem. Soc.*, 2012, **134**, 10047; e) O. J. Cooper, D. P. Mills, J. McMaster, F. Tuna, E. J. L. McInnes, W. Lewis, A. J. Blake, S. T. Liddle, *Chem. Eur. J.*, 2013, **19**, 7071.
8. S. T. Liddle, D. P. Mills, A. J. Wooles, *Chem. Soc. Rev.*, 2011, **40**, 2164.
9. a) S. T. Liddle, J. McMaster, J. C. Green, P. L. Arnold, *Chem. Commun.*, 2008, 1747; b) D. P. Mills, O. J. Cooper, J. McMaster, W. Lewis, S. T. Liddle, *Dalton Trans.*, 2009, 4547; c) S. T. Liddle, D. P. Mills, B. M. Gardner, J. McMaster, C. Jones, W. D. Woodul, *Inorg. Chem.*, 2009, **48**, 3520; d) D. P. Mills, A. J. Wooles, J. McMaster, W. Lewis, A. J. Blake, S. T. Liddle, *Organometallics*, 2009, **28**, 6771; e) A. J. Wooles, D. P. Mills, W. Lewis, A. J. Blake, S. T. Liddle, *Dalton Trans.*, 2010, **39**, 500; f) A. J. Wooles, O. J. Cooper, J. McMaster, W. Lewis, A. J. Blake, S. T. Liddle, *Organometallics*, 2010, **29**, 2315; g) D. P. Mills, L. Soutar, W. Lewis, A. J. Blake, S. T. Liddle, *J. Am. Chem. Soc.*, 2010, **132**, 14379; h) D. P. Mills, W. Lewis, A. J. Blake, S. T. Liddle, *Organometallics*, 2013, **32**, 1239; i) D. P. Mills, L. Soutar, O. J. Cooper, W. Lewis, A. J. Blake, S. T. Liddle, *Organometallics*, 2013, **32**, 1251.
10. a) R. R. Schrock, *J. Am. Chem. Soc.*, 1976, **98**, 5399; b) R. R. Schrock, *Chem. Rev.*, 2001, **102**, 145; c) R. R. Schrock, *Chem. Rev.*, 2009, **109**, 3211.
11. F. H. Allen, CSD version 5.33 - November 2011, *Acta Crystallogr. Sect. B*, 2002, **58**, 380.
12. O. P. Lam, C. Anthon, F. W. Heinemann, J. M. O'Connor, K. Meyer, *J. Am. Chem. Soc.*, 2008, **130**, 6567.
13. B. O. Roos, P. Pykkö, *Chem. Eur. J.*, 2010, **16**, 270.
14. A) O. P. Lam, F. W. Heinemann, K. Meyer, *Chem. Sci.* 2011, **2**, 1538; b) B. M. Gardner, J. C. Stewart, A. L. Davis, J. McMaster, W. Lewis, A. J. Blake, S. T. Liddle, *Proc. Natl. Acad. Sci. USA* 2012, **109**, 9265.
15. a) R. P. Kamalesh Babu, R. McDonald, R. G. Cavell, *Organometallics*, 2000, **19**, 3462; b) R. G. Cavell, R. P. K. Babu, K. Aparna, *J. Organomet. Chem.*, 2001, **617-618**, 158.

16. R. G. Pearson, *J. Chem. Educ.*, 1968, **45**, 581.

17. J. C. Berthet, M. Ephritikhine, *Coord. Chem. Rev.*, 1998, **178-180**, 83-116.

Figures and Captions



Scheme 1. Synthesis of **2-8**. Reagents and conditions: (i) Ph_2CO or PhCHO , THF; (ii) Bu^tCOPh , toluene; (iii) coumarin, THF; (iv) PhCOF , toluene; (v) Bu^tNCO , toluene; (vi) $\text{C}(\text{NCy})_2$, toluene. Formal charges for **5** are omitted for clarity.

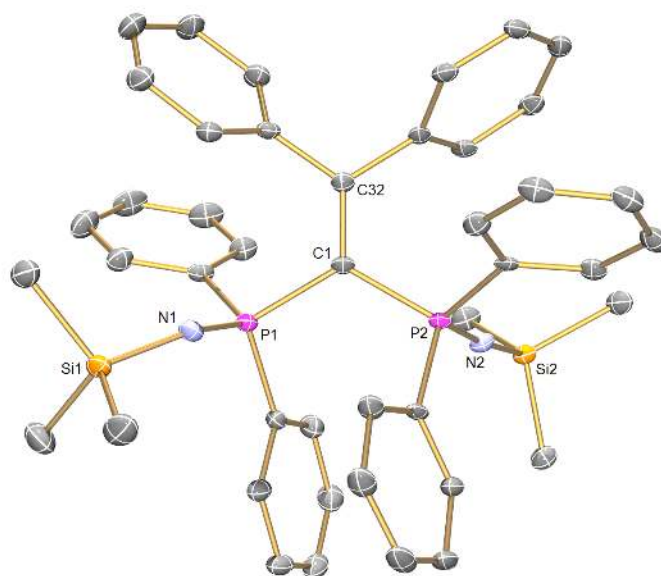


Figure 1. Molecular structure of of **2** with selective labelling and displacement ellipsoids set to 30%. Hydrogen atoms and lattice solvent are omitted for clarity. Two molecules of **2** crystallise in the asymmetric unit but they are very similar so only one molecule is described. Selected bond lengths [Å] and angles [°] for **2**: C1-C32 1.359(4), C1-P1 1.837(3), C1-P2 1.831(3), P1-N1 1.535(2), P2-N2 1.535(3); P1-C1-P2 119.49(15).

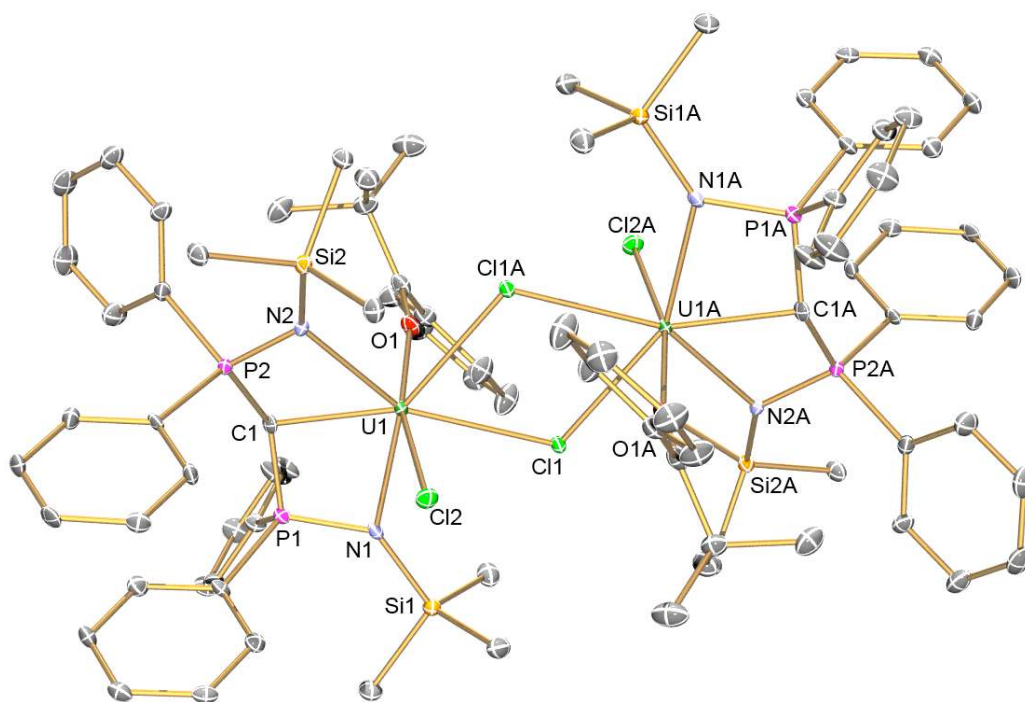


Figure 2. Molecular structure of **3** with selective labelling and displacement ellipsoids set to 30%. Hydrogen atoms and lattice solvent are omitted for clarity. Selected bond lengths [Å] and angles [°] for **3**: U1–C1 2.346(4), U1–N1 2.433(3), U1–N2 2.423(3), U1–Cl1 2.8471(9), U1–Cl2 2.6223(10), U1–O1 2.453(3), C1–P1 1.675(4), C1–P2 1.672(4), P1–N1 1.621(4), P2–N2 1.621(4), O1–C32 1.239(6); P1–C1–P2 144.6(3).

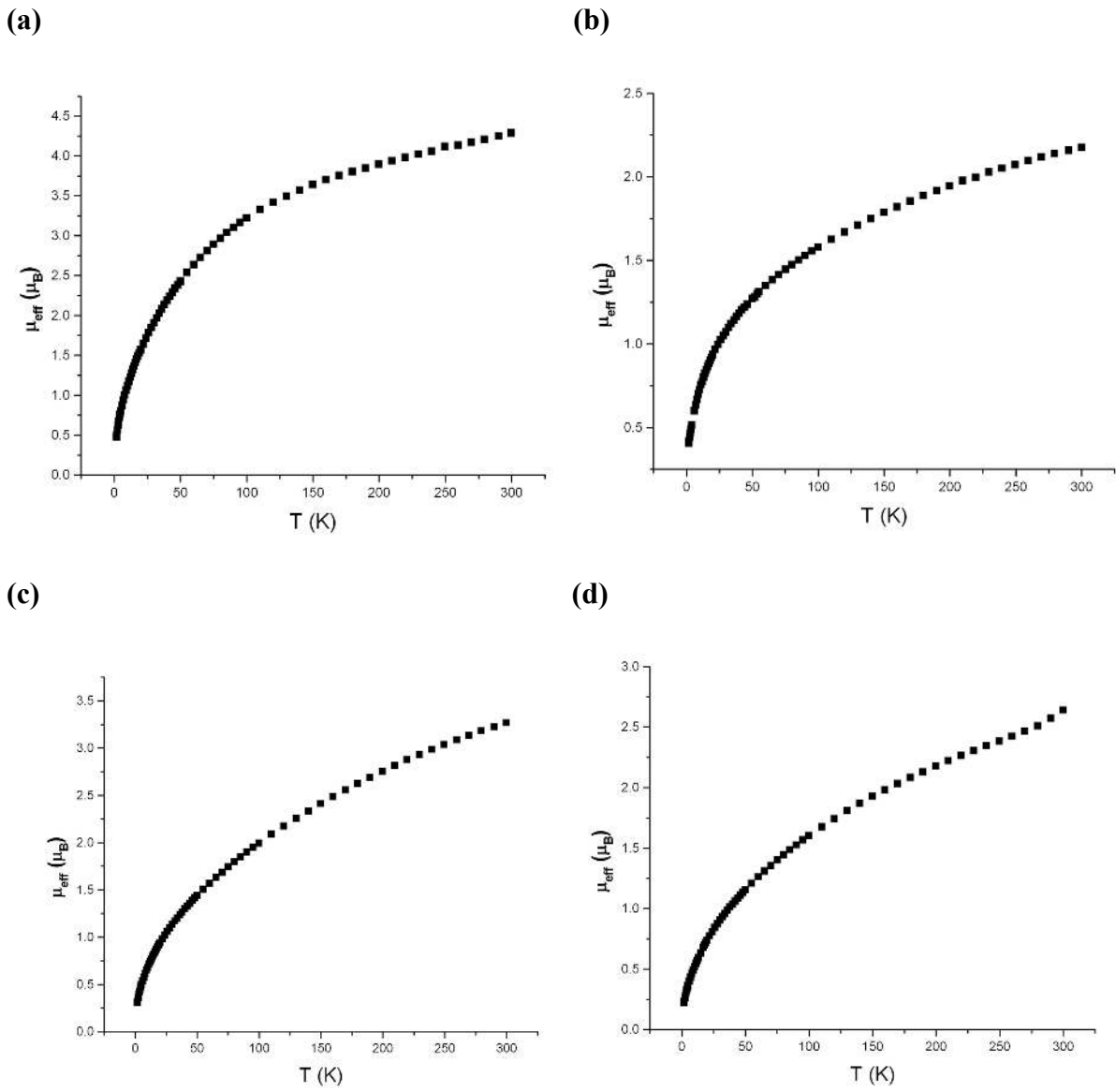


Figure 3. Variable temperature $\mu_{\text{eff}}(\mu_B)$ vs. T (K) data for (a) **3**, (b) **4**, (c) **7**, and (d) **8**.

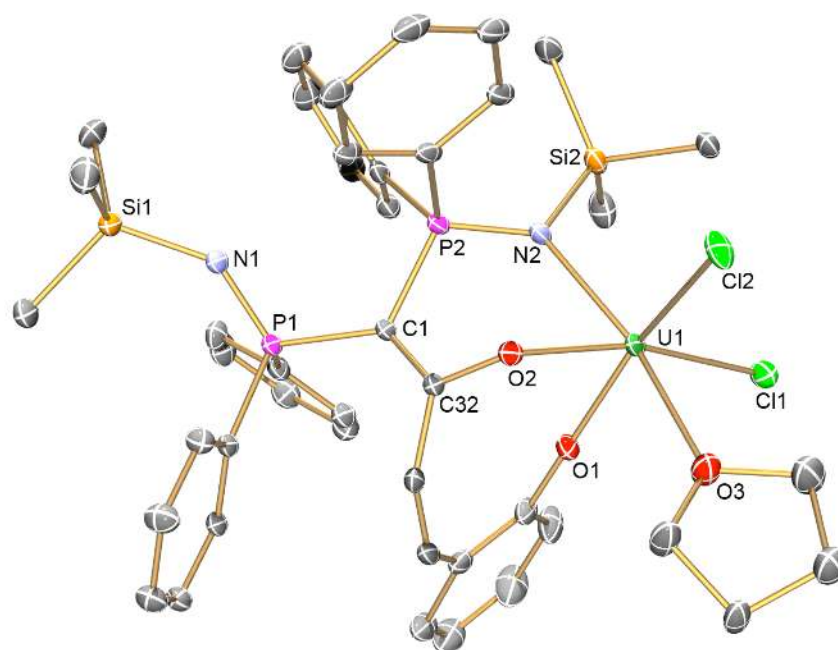


Figure 4. Molecular structure of **4** with selective labelling and displacement ellipsoids set to 30%. Hydrogen atoms and lattice solvent and coumarin omitted for clarity. Selected bond lengths [Å] and angles [°] for **4**: U1–O1 2.089(3), U1–O2 2.213(3), U1–O3 2.416(4), U1–Cl1 2.6604(13), U1–Cl2 2.6299(13), U1–N2 2.394(4), C1–C32 1.361(7), C1–P1 1.823(5), C1–P2 1.809(5), O2–C32 1.335(6), P1–N1 1.541(4), P2–N2 1.616(4), C33–C34 1.330(8); P1–C1–P2 118.3(3), O1–U1–O2 79.52(13).

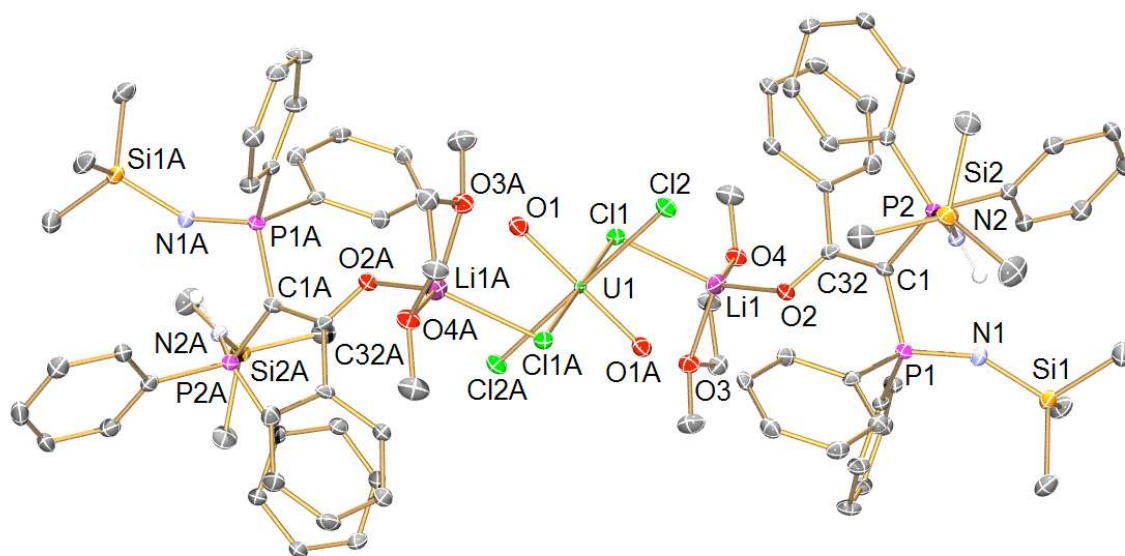


Figure 5. Molecular structure of **5** with selective labelling and displacement ellipsoids set to 30%. Hydrogen atoms (except those on N2 and N2A), minor disorder components and lattice solvent are omitted for clarity. Selected bond lengths [Å] and angles [°] for **5**: U1–O1 1.759(5), U1–Cl1 2.7001(15), U1–Cl2 2.6551(15), Li1–Cl1 2.372(12), Li1–O2 1.870(12), Li1–O3 2.021(13), Li1–O4 1.979(12), O1–C32 1.269(8), C1–C32 1.416(9), C1–P1 1.782(6), C1–P2 1.755(6), P1–N1 1.562(5), P2–N2 1.641(6); P1–C1–P2 112.9(3).

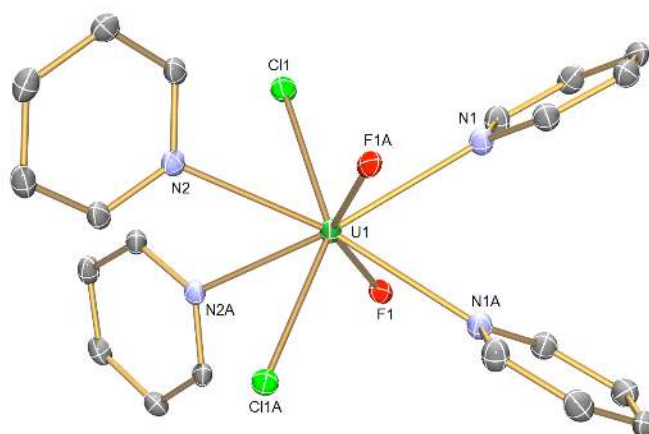


Figure 6. Molecular structure of **6** with selective labelling and displacement ellipsoids set to 30%. Hydrogen atoms, minor disorder components and lattice solvent are omitted for clarity. Selected bond lengths [Å] for **6**: U1–F1 2.1592(17), U1–Cl1 2.6969(12), U1–N1 2.649(2), U1–N2 2.709(2).

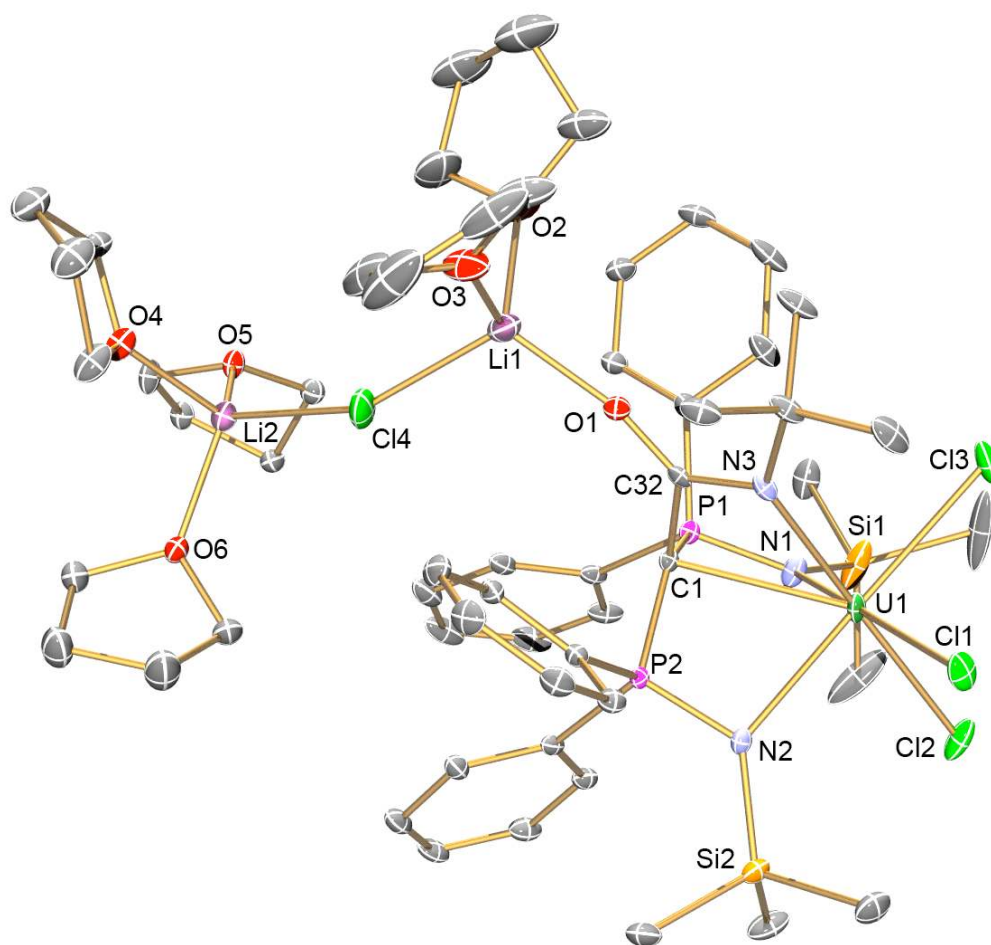


Figure 7. Molecular structure of **7** with selective labelling and displacement ellipsoids set to 30%. Hydrogen atoms, minor disorder components and lattice solvent are omitted for clarity. Selected bond lengths [Å] and angles [°] for **7**: U1–C1 2.634(3), U1–N1 2.500(3), U1–N2 2.411(3), U1–N3 2.451(3), U1–Cl1 2.6569(10), U1–Cl2 2.6382(8), U1–Cl3 2.6635(9), C1–C32 1.512(4), C1–P1 1.743(3), C1–P2 1.751(3), N3–C32 1.334(4), O1–C32 1.242(4), P1–N1 1.598(3), P2–N2 1.611(3); P1–C1–P2 126.83(17), N1–U1–N2 96.19(9), N3–C32–O1 128.3(3).

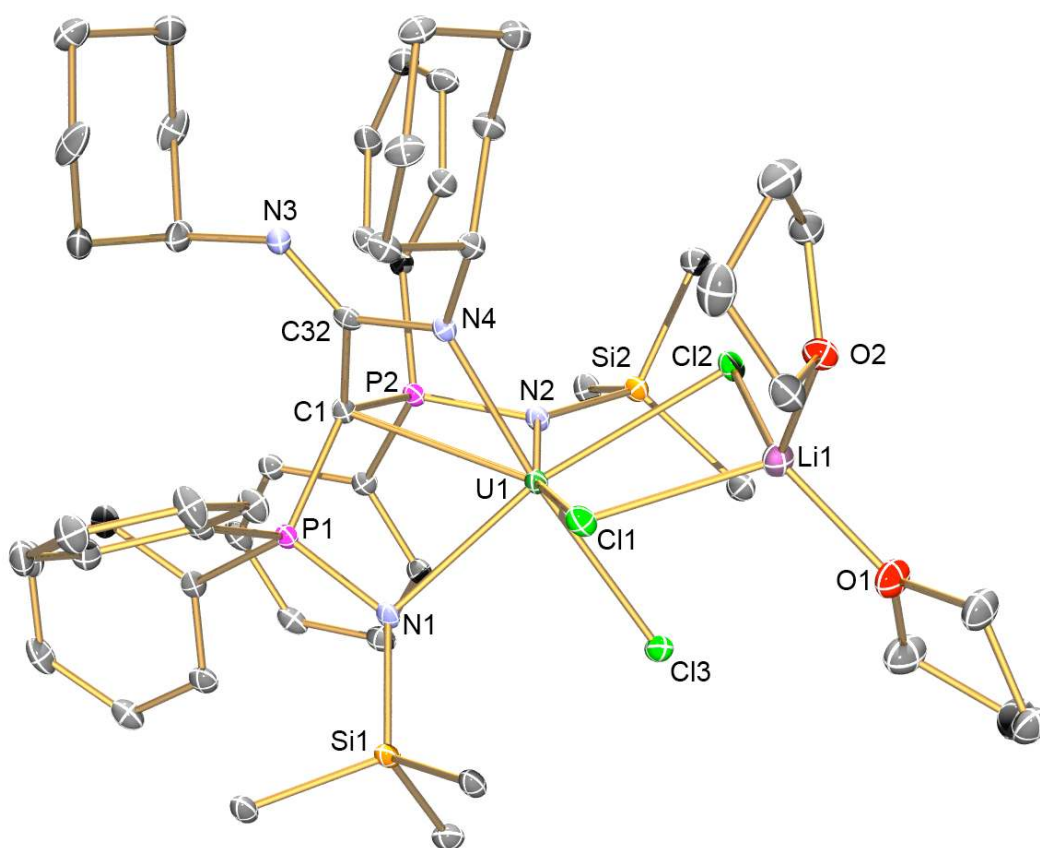
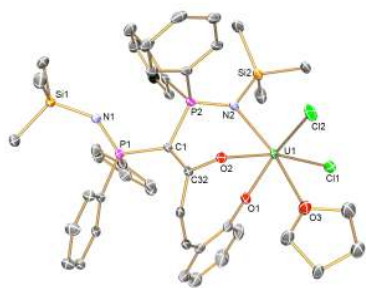


Figure 8. Molecular structure of **8** with selective labelling and displacement ellipsoids set to 30%. Hydrogen atoms omitted for clarity. Selected bond lengths [Å] and angles [°] for **8**: U1–C1 2.712(5), U1–N1 2.456(4), U1–N2 2.376(4), U1–N4 2.296(4), U1–Cl1 2.7615(12), U1–Cl2 2.7674(12), U1–Cl3 2.6433(13), C1–C32 1.525(7), C1–P1 1.765(5), C1–P2 1.753(5), N3–C32 1.273(6), N4–C32 1.388(6), P1–N1 1.606(4), P2–N2 1.621(4); P1–C1–P2 121.2(3), N1–U1–N2 98.59(14), N3–C32–N4 123.6(5).

ToC



Metallo-Wittig, adduct formation, C-F bond activation, and [2 + 2]-cycloaddition reactivities of a uranium(IV)-carbene towards carbonyls and heteroallenes are described.